ORIGINAL RESEARCH PAPER

Radio-Diagnosis

KEY WORDS: Magnetic Resonance Imaging, Dynamic Contrast Enhanced Magnetic Resonance Imaging, Diffusion Weighted Imaging, Apparent Diffusion Coefficient, The Ovarian-Adnexal Reporting and Data System, Total Relative Enhancement, Time to Peak, Ultrasonography

# ROLE OF FUNCTIONAL MRI AND O-RADS MRI RISK SCORE IN EVALUATION OF INDETERMINATE OVARIAN MASSES

**Prof. (Dr) Karuna Hazarika** M.D., DMRD, Professor and Head, Department of Radio-Diagnosis, Tezpur Medical College and Hospital, Assam

**Dr. Halimuddin Ahmed** M.D., Assistant Professor, Department of Radio-Diagnosis, Tezpur Medical College and Hospital, Assam

**Dr. Md Mohidul Islam*** Post-Graduate Trainee, Department of Radio-Diagnosis, Tezpur Medical College and Hospital, Assam *Corresponding Author

ABSTRACT

**Background-** Ovarian masses are a common finding in routine clinical practice. MRI shows great accuracy in the detection and discrimination of ovarian/adnexal masses, but conventional MRI sequences sometimes fail to characterize indeterminate ovarian masses. Functional MRI techniques, such as DWI and DCE-MRI provides further information based on tissue cellularity and internal architecture of ovarian tumors respectively. **Aims-**To evaluate the various conventional and DCE-MRI characteristics of ovarian masses, to estimate their ADC values and to assess the performance of the O-RADS MRI risk score. **Materials and methods-** The study was conducted in the Department of Radio-diagnosis, TMCH over a period of one year, on 50 patients diagnosed with indeterminate or suspicious ovarian mass in US examination. MRI was performed on a 1.5-T MR imaging unit. The findings were correlated with results of HPE. **Results-** The diagnostic accuracy of O-RADS MRI risk score was 93.2%, sensitivity 94.74%, and specificity 93.67%. Among the DCE-MR parameters, MRE% showed higher specificity (80%) and Tmax showed higher sensitivity (97.5%). Malignant masses showed higher MRE% and less time to peak compared to benign masses. ADC cut-off of <1.0x10-3 for the solid component of the masses has produced a sensitivity of 90.24%, specificity of 77.78% and accuracy of 88.5%. **Conclusion-** Based on the results of our study, we conclude that in cases of indeterminate ovarian masses, functional MRI should be the investigation of choice. Further, applying the O-RADS MRI risk score in clinical practice standardizes reporting and allows for a customized patient-centred strategy.

## INTRODUCTION:

Ovarian masses are a common finding in routine clinical practice. Even though most ovarian masses are benign, malignant variants pose a significant public health threat. Ovarian carcinoma is the third most prevalent cancer among Indian women, after breast and cervical cancer, according to GLOBOCAN 2020 report.[1] Most women are detected in the late stages of the disease due to the absence of symptoms in the early stages, with five-year survival rates of about 30–50%.[2] Characterization of ovarian masses and preoperatively differentiating benign, borderline, and malignant tumors is very important in order to plan adequate therapeutic procedures. Imaging methods have a vital role in the detection, characterization, and staging of ovarian masses. The initial imaging modality for the characterization of adnexal masses is ultrasonography because it is economical and radiation-free. Recently, significant effort has been put to enhance the presurgical identification of adnexal tumors by creating risk models and sonographic scoring systems. After sonography, 5 to 25 percent of adnexal lesions in clinical practice will still be indeterminate.[3] Even using the International Ovarian Tumor Analysis group (IOTA) simple rules, 22 % of lesions remained indeterminate on ultrasound (US).[4] The majority of these turn out to be common benign entities such as ovarian fibromas, broad ligament fibroids, fat-poor mature teratomas, and hemorrhagic lesions.

Certain cases can be staged with computed tomography and referred to a gynecologic oncology centre since they are clearly malignant. The most common gynecologic indication for magnetic resonance imaging (MRI) is sonographically indeterminate ovarian tumors. The excellent soft tissue resolution of MRI makes it a particularly favoured method. The number of indeterminate cases is decreased by using MRI as a secondary test since it lowers the false positive rate for malignancy. As a result, MRI prevents benign lesions from undergoing unnecessary surgery and enables the proper referral of lesions with a moderate to high positive predictive value for cancer to gynecologic oncology. Although MRI shows excellent accuracy in the detection and discrimination of adnexal masses, conventional MRI sequences sometimes fail to characterize ovarian masses. Functional MRI techniques, such as diffusion-weighted MRI (DWI) and dynamic contrast-enhanced (DCE) perfusion, have recently been incorporated into medical practice in addition to standard MRI sequences. Using DWI, which measures the diffusivity of endogenous water molecules in tissue and reflects the mean size of the tissue microstructure that restricts and/ or hampers the Brownian random motion of water molecules, it is possible to distinguish between benign and malignant lesions.[5] The logarithmic response of diffusion images is known as the apparent diffusion coefficient (ADC). Restricted diffusion is evaluated semi-quantitatively and expressed as a map or a number. Cancers have shown increased ADC values in gynecologic applications of diffusion-weighted MR imaging.[6] Using serial images, the DCE T1-weighted perfusion MRI technique assesses signal alterations in tissue following the intravenous administration of a contrast agent. The T1 relaxation time affects the signal dynamics after contrast injection.

The increase in signal intensity depends on the degree of enhancement due to the paramagnetic contrast agent's T1 shortening effect. For accurate internal architecture characterization of ovarian tumors, DCE-MRI is advised, particularly for delineating necrosis, papillary projections, solid components, septations, and peritoneal implants.[7] It offers details on the vascularity and perfusion of the tumor. Additionally, extra post-processing quantitative data is provided.

The Ovarian-Adnexal Imaging-Reporting-Data System MRI (O-RADS MRI) was created by American College of Radiology (ACR) to streamline and standardize the reporting of MRI of adnexal masses in order to give the clinician the information required for the most appropriate management of patients. In the O- RADS MRI score[8], the absence of a suspicious adnexal lesion is given a score of 1; an adnexal lesion that is almost is

certainly benign given a score of 2; a low-risk lesion attributed a score of 3; an intermediate-risk lesion receives a score of 4, and a high-risk lesion is coded with a score of 5.

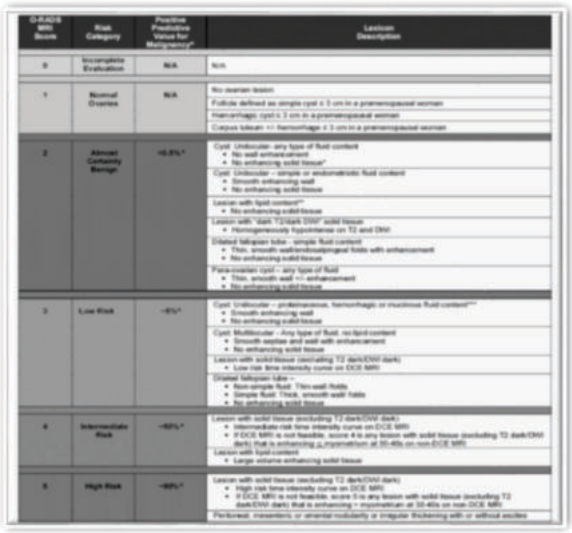

**Fig 1: O-RADS MRI Risk Stratification and Management System**[8]

In their study, Thomassin-Naggara et al. found that, for the detection of malignant ovarian masses, a ORADS-MRI score of 4 and 5 had a sensitivity of 93.0% and a specificity of 91.0%.[9] There are fewer studies assessing the diagnostic performance of ORADS-MRI in India. Hence, the aim of this study was to assess the diagnostic performance of the ORADS-MRI scoring system along with functional MRI in sonographically indeterminate ovarian masses by using histopathology as the reference standard.

## AIM AND OBJECTIVES:

To evaluate the various conventional and DCE-MRI characteristics of ovarian masses, to estimate their ADC values and to assess the performance of the O-RADS MRI risk score.

## MATERIALS AND METHODS:

This hospital based prospective study was conducted in the Department of Radio-diagnosis, Tezpur Medical College, and Hospital over a period of one year, on 50 patients diagnosed with indeterminate or suspicious ovarian mass in US examination. The ethical approval was obtained from Institutional Human Ethical Committee (No. 056/2021/TMCH) and written informed consent was taken from all patients.

### Inclusion criteria-

- Indeterminate and suspicious malignant ovarian masses detected in USG.

### Exclusion criteria-

- <7 years of age.
- Ovarian masses with typical benign features on ultrasonography, like simple cysts, hemorrhagic cysts, dermoid, and endometrioma, were excluded.
- Patients with metallic implants, prostheses, aneurysm clips, pacemakers, Claustrophobic patients & gadolinium contrast-sensitive patients.

### MR imaging-

### Patient preparation

Patients were instructed to fast for three hours and void urine two hours prior to the examination. To reduce intestinal peristalsis, an antispasmodic medication (20 mg of buscopan) was administered intravenously just before MR imaging.

### MRI protocol

MR imaging was done on a 1.5-T MR imaging machine (Ingenia, Philips medical system). All the patients were scanned in the supine position using a pelvic phased-array Torso coil.

**Table1:The MRI protocol used in the study.**

| Sequence | TR(ms) | TE(ms) | Slice thickness(mm) | FOV AP (mm)xRL(mm)xFH(mm) | Matrix | Flip angle | Fat saturation |
|---|---|---|---|---|---|---|---|
| Axial T1 | 400-600 | 8 | 3.5 | 220x192x154 | 276x149 | 90 | Fat sat |
| Axial T2 | 3000-5000 | 90 | 3.5 | 220x192x154 | 276x149 | 90 | Fat sat |
| Sagittal T1 | 400-600 | 8 | 2.5 | 240x240x148 | 240x240 | 90 | - |
| Sagittal T2 | 3000-5000 | 100 | 2.5 | 240x240x148 | 240x240 | 90 | - |
| Coronal T1 | 400-600 | 10 | 2.5 | 210x210x110 | 248x170 | 90 | - |
| Coronal T2 | 3000-5000 | 90 | 2.5 | 210x210x110 | 248x170 | 90 | - |
| DWI (b value of 400 &800) | - | - | 0.4 | 220x192x154 | 72x64 | 90 | - |
| e THRIVE | Shortest | Shortest | 0.4 | 250x197x140 | 168x114 | 10 | - |

- DW-MRI was acquired in the axial plane before administering the contrast medium using a single-shot echoplanar imaging sequence with b value 400s/mm$^2$ and 800s/mm$^2$. Multiple b-values were obtained to reduce the error in ADC calculation and improve tissue characterization.
- DCE-MRI: Post-contrast T1 fat sat THRIVE (High-Resolution Isotropic Volume Examination) images were obtained immediately after injecting gadopentate dimeglumine at a dose of 0.1 mmol/kg of body weight, at a rate of 3-4ml/sec followed by flushing of 20 mL of normal saline in the infusion pump. Images were obtained every 15-20 secs. Finally, transverse, sagittal and coronal T1-weighted gradient-echo images were acquired.

### MR imaging analysis-

MR images were analysed for the following:
MR appearance of the tumor; either unilocular or multilocular cystic, solid components, involvement of one or both ovaries, size of the lesions, signal intensity of the tumor, enhancement of the solid components if present, thickness and regularity of wall of the tumor and its enhancement, presence of vegetation and septations, their enhancement pattern and their size. MR images were also looked for the presence of ascites and the presence of peritoneal and omental deposits.

### DW-MRI analysis-

### Qualitative analysis

The lesions were analysed for low signal intensity on diffusion images with high signal in the corresponding ADC maps (facilitated) and high signal intensity on diffusion images with lowering of the signal in the corresponding ADC maps (restricted diffusion).

### Quantitative analysis

Regarding the quantitative analysis of DWI, the ADC map was generated, and then ROI (region of interest) was selected manually on the solid and the cystic component of the tumors, which was then automatically calculated on the workstation to get the ADC values.

### DCE-MRI semi-quantitative analysis-

Analysis was done using Philips IntelliSpace Portal IX V10.1.1

windows workstation. ROI was placed manually within the greatest enhancing solid areas of the ovarian masses on subtracted enhanced series. ROI size ranged from 10-150 $mm^2$. The following dynamic parameters were recorded:

- "Enhancement amplitude" is automatically calculated as the Maximum relative enhancement percentage (MRE%)."
- Time to peak- Tmax" including early (two phases post uptake ≤120 sec.) and delayed (three phases prior to the end of examination ≥200 sec.) peaks of contrast uptake.
- "Time/ signal intensity curves"- automatically generated at the workstation. It is calculated at the point of abrupt decline in the Tmax elicited by the time/ signal intensity curve.

The final diagnosis was made using the terminology in the ACR ORADS-MR lexicon 2021, and were finally classified into O-RADS MRI scores of 1- 5

**Reference standard-**

The patients were followed up in the Department of Obstetrics and Gynecology; TMCH and MRI diagnosis was correlated with post-operative histopathology results.

**Statistical methods-**

To describe the data, descriptive statistics, including frequency analysis and percentage analysis, were used for categorical variables, and the mean and standard deviation were used for continuous variables. Characteristic MRI findings of the pathologies were assessed individually concerning the relationship with its final diagnosis using the Chi-square test for categorical variables considering a p-value of less than 0.05 as significant. All statistical calculations were done using the computer programme SPSS (Statistical package for the social science; SPSS Inc., Chicago, USA) software for windows version 25.0 The Receiver Operator Characteristic (ROC) curve analysis was done to find the sensitivity, specificity, PPV, NPV and accuracy of O-RADS MRI, DCE parameters, and mean ADC value taking HPE results as the gold standard. We calculated the sensitivity, specificity, positive predictive value, and negative predictive value for O-RADS MRI scores, using ≥ 4 as the cut-off score for malignancy.

**RESULTS AND DISCUSSION:**

The patients' age ranged from 21 years to 65 years (mean age 47 ± 12). The mean age of malignant ovarian masses, benign masses, and borderline were 49±11 years, 40±14 years, and 47±13 years respectively.

Unilateral masses were more common than bilateral ovarian masses. Among 50 patients, 42 (84%) cases were unilateral, and bilateral ovarian masses were found in 8 (16%) patients. In case of bilateral ovarian masses, each lesion was separately characterized, and the lesion with the highest score was considered. The majority of bilateral ovarian masses were proved malignant on HPE. (Figure: 3)

Among 50 studied patients, 47 cases (94%) had lesions that were of ovarian origin and the rest, 3 (6%), were of extra-ovarian origin (2 cases of tubo-ovarian abscesses and 1 case of broad ligament fibroid). (Table: 8) The origin of these lesions could not be determined on USG because of larger size and complex appearance, which MRI did and classified them into O-RADS risk score accordingly.

MRI characterization showed that ovarian masses, which are solid, solid-cystic with enhancing solid components, thick irregular enhancing septa/ wall, ascites, and peritoneal/ mesenteric/ omental deposits, were highly malignant. This is consonant with the findings of Sohaib et al. in 2007. They concluded that MRI findings suggestive of malignancy include the demonstration of solid masses, solid-cystic masses, and the presence of papillary projections and thick septa in the cyst wall.[10] In our study, MRI detected solid components in all malignant cases. Maximum (n=31, 86.1%) malignant lesions were multilocular cystic lesions with a solid component. 4 (11.1%) malignant lesions were predominantly solid. One malignant lesion was unilocular cystic with papillary projection and enhancing mural nodule. (Figure: 2) 4 (80%) of 5 borderline ovarian masses were multilocular cystic lesions with a solid component.

In our study, 31 out of 35 malignant primary ovarian lesions were multilocular which is broadly comparable with the results of the study by **Brown et al.** in 2010 who found 40 out of 54 primary ovarian cancers multilocular.[11] (Table: 2)

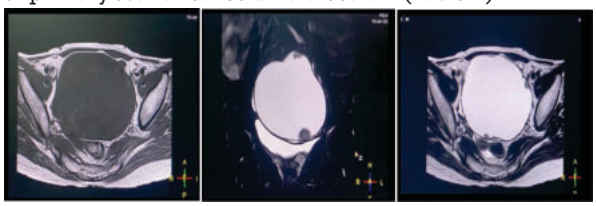

**(A) Axial T1** **(B) Coronal T2** **(C) Axial T2**

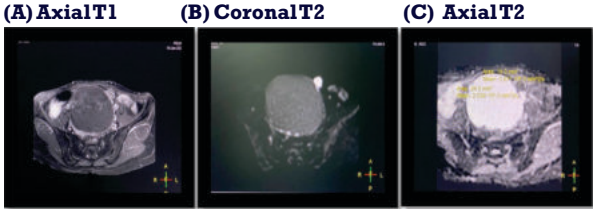

**(D) T1+C** **(E) DWI** **(F) ADC**

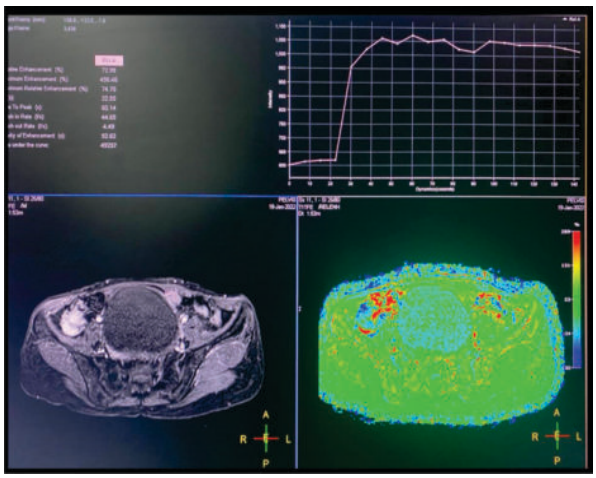

**(G) DCE-MRI with colour mapping and time-intensity curve.**

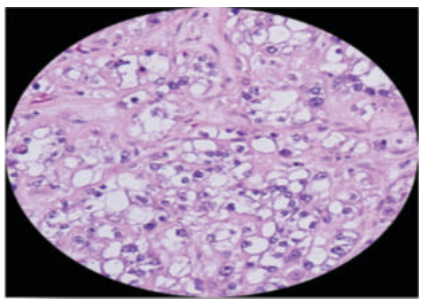

**(H) HPE-Right ovarian clear cell carcinoma.**

**Figure 2: Axial and coronal T2WI show a unilocular cystic lesion with papillary projection and a mural nodule that appears intermediate in signal intensity. T1+C shows vivid enhancement of the mural nodules. Mild ascites seen. DWI shows restriction with a low ADC value. DCE-MR shows a type 3 curve. MRE=74.7%, Tmax=60.1s. MRI diagnosis: O-RADS 5 lesion.**

**Table 2: Distribution of lesions based on various MRI parameters and cross tabulation with HPE findings.**

| MRI parameters | | HPE Category | | | | | | | | p-value |
|---|---|---|---|---|---|---|---|---|---|---|
| | | Benign | | Borderline | | Malignant | | Total | | |
| | | No. | % | No. | % | No. | % | No. | % | |
| Laterality | Bilateral | 1 | 11.10% | 0 | 0.00% | 7 | 19.40% | 8 | 16.00% | 0.468 |
| | Unilateral | 8 | 88.90% | 5 | 100.00% | 29 | 80.60% | 42 | 84.00% | |
| content of ovarian masses | Multilocular cystic lesion | 1 | 11.10 | 0 | 0.00 | 0 | 0.00 | 1 | 2.00 | 0.023 |
| | Multilocular cystic lesion with solid component | 3 | 33.30 | 4 | 80.00 | 31 | 86.10 | 38 | 76.00 | |
| | Solid | 3 | 33.30 | 0 | 0.00 | 4 | 11.10 | 7 | 14.00 | |
| | Unilocular cystic lesion | 1 | 11.10 | 0 | 0.00 | 0 | 0.00 | 1 | 2.00 | |
| | Unilocular cystic with solid component | 1 | 11.10 | 1 | 20.00 | 1 | 2.80 | 3 | 6.00 | |
| septal characteristics (septal thickness) | Absent | 4 | 44.40 | 1 | 20.00 | 4 | 11.10 | 9 | 18.00 | 0.037 |
| | <3 mm | 2 | 22.20 | 1 | 20.00 | 1 | 2.80 | 4 | 8.00 | |
| | >3 mm | 3 | 33.30 | 3 | 60.00 | 31 | 86.10 | 37 | 76.00 | |
| T2WI signal intensity of the masses | Hyperintense | 4 | 44.40 | 4 | 80.00 | 9 | 25.00 | 17 | 34.00 | 0.015 |
| | Hypointense | 3 | 33.30 | 0 | 0.00 | 0 | 0.00 | 3 | 6.00 | |
| | Intermediate | 2 | 22.20 | 1 | 20.00 | 27 | 75.00 | 30 | 60.00 | |
| time/ signal intensity curve on DCE-MRI | Type1 | 8 | 88.90 | 1 | 20.00 | 1 | 2.80 | 10 | 20.00 | 0.002 |
| | Type 2 | 1 | 11.10 | 4 | 80.00 | 17 | 47.20 | 22 | 44.00 | |
| | Type 3 | 0 | 0.00 | 0 | 0.00 | 18 | 50.00 | 18 | 36.00 | |
| Ascites | Absent | 8 | 88.90 | 4 | 80.00 | 6 | 16.70 | 18 | 36.00 | 0.001 |
| | Present | 1 | 11.10 | 1 | 20.00 | 30 | 83.30 | 32 | 64.00 | |
| Peritoneal, mesenteric or omental nodularity or irregular thickening | Absent | 9 | 100.00 | 5 | 100.00 | 25 | 69.40 | 39 | 78.00 | 0.001 |
| | Present | 0 | 0.00 | 0 | 0.00 | 11 | 30.60 | 11 | 22.00 | |

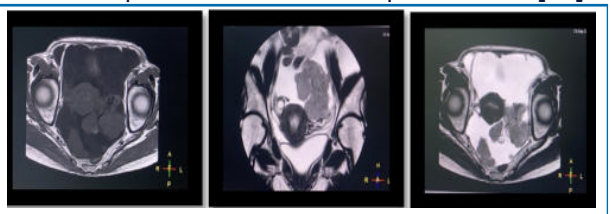

(A) Axial T1 (B) Coronal T2 (C) Axial T2

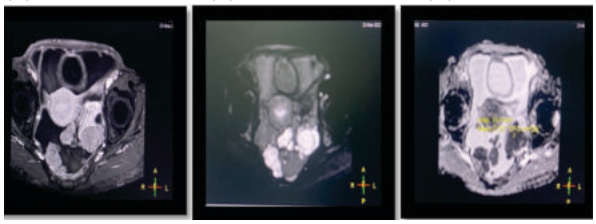

(D) T1+C (E) DWI (F) ADC

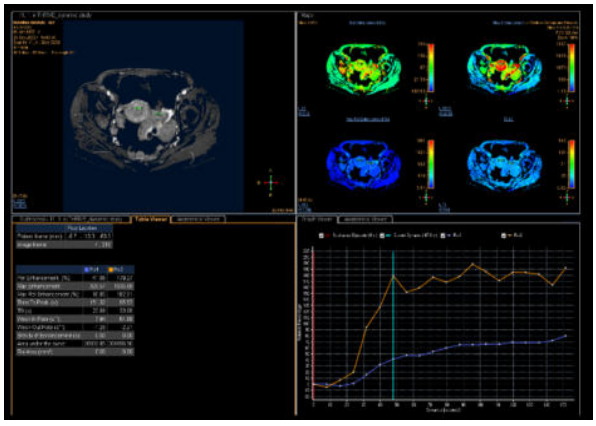

(G) DCE-MRI with colour mapping and time-intensity curve.

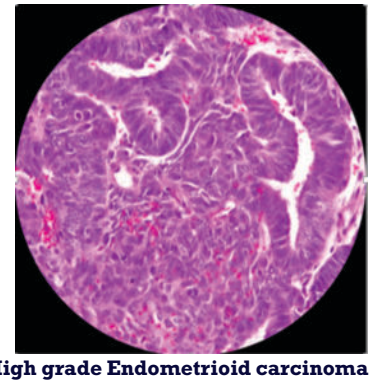

(H) HPE-High grade Endometrioid carcinoma of bilateral ovaries.

**Figure 3: Axial and coronal MR images show bilateral solid ovarian masses which appear hypointense and intermediate signal intensity on T1 and T2WI respectively. T1+C shows heterogeneous enhancement of the lesions along with enhancing peritoneal deposits. Moderate ascites seen. DWI shows restriction with a low ADC value. DCE-MR shows a type 3 curve. MRE= 182.9%%, Tmax=95.5s.**

**MRI Diagnosis: Bilateral O-RADS 5 lesions.**

Masses of intermediate signal intensity on T2WI comprised 60%. 27 (75%) malignant masses showed intermediate T2 signal intensity, while 9 (25%) malignant masses showed hyperintense T2 signal intensity.

All T2 hypointense masses were proved benign on HPE. These were DWI dark lesions. 4 (80%) borderline masses showed hyperintense T2 signal. (Table: 2) Findings are broadly in agreement consistent with the study by Mansour et al. in 2015,

where they found that intermediate SI on T2WI is more common in invasive carcinomas than benign and borderline masses.[12]

The DW-MRI is a crucial tool that enables the radiologist to shift from morphological to functional assessment of disorders of the female pelvis. In this study, 90% of the lesions showed restricted diffusion (hyperintense signal in DWI and hypointense in ADC map), whereas 10% displayed facilitated diffusion. All malignant (n = 36, 100%) and three of the borderline lesions (n = 3, 60%), as well as 6 (66.7%) benign lesions showed restricted diffusion. It is well known that DWI gives false positive results in benign lesions where there are non-cellular, highly concentrated molecular components such as debris and caseous materials. In our study: 2 TOAs, one broad ligament fibroid and one hemorrhagic cyst are among the benign lesions that showed a false positive result on DWI.

Regarding the mean ADC values, we found that the solid components for the benign lesions differed significantly from that of the borderline and malignant lesions ($P \leq 0.001$). The mean ADC value of solid component is shown in table 3.

We conclude that ADC measurement in the solid components was more accurate in identifying benign and malignant lesions. This agrees with a study carried out by Li et al. in 2017. They concluded that solid components with high or low signal intensity on T2-weighted images and restriction on DWI with low ADC values (less than $1.20 \times 10^{-3}$ mm$^2$/s) at high b values indicate malignant masses.[13]

**Table 3: Mean values of Semi-quantitative DCE-MRI parameters and ADC**

| MRI parameters | | HPE Category | | | | | | P-value |
|---|---|---|---|---|---|---|---|---|
| | | Benign | | Borderline | | Malignant | | |
| | | Mean | Standard deviation | Mean | Standard deviation | Mean | Standard deviation | |
| Semi-Quantitative DCE-MRI Parameters | Tmax (s) | 154.4 | 28.3 | 121.5 | 17.1 | 91.2 | 28.3 | 0.001 |
| | MRE % | 77.4 | 46.2 | 109.6 | 35.3 | 148.7 | 39.6 | |
| Mean ADC value x10-3 | Solid components of lesion | 1.23 | 0.38 | 1.30 | 0.43 | 0.74 | 0.16 | 0.001 |
| | Cystic components of lesion | 2.14 | 0.50 | 2.22 | 0.37 | 2.44 | 0.26 | 0.012 |

Additionally, there was statistical significance between the mean ADC values of the cystic components of the benign and malignant lesions in the current study ($P = 0.012$). It might be explained by the inclusion of TOA cases with cyst contents with low ADC values.

In our study, the ADC value was the more accurate tool. This is unlike the analysis done by Thomassin-Naggara et al. in 2009, where they characterized 77 adnexal masses using DWI. They considered the signal intensity at the DWI to be the accurate tool for predicting benign and malignant criteria, not the ADC values.[14]

In our study, TOAs posed a particular challenge because their cystic components displayed significant signals on the DWI with low ADC values ($0.8\times 10^{-3}$ mm$^2$/s in the ADC maps), creating the appearance of a malignant tumor. However, these lesions can be identified with a thorough clinical history and tumor markers. TAOs further showed smooth peripheral rim enhancement in the post-contrast study, which helped in easy identification.

Although the hemorrhagic cyst and the broad ligament fibroid showed intermediate to high signals in DWI with low ADC values, they were reliably identified as benign based on T1 and T2 SI.

Five borderline ovarian tumors that appeared differently on DWI were present. Two cases showed facilitated diffusion with a high ADC value, pointing to benign disease (false negative). Three cases showed restricted diffusion with high signal on DWI and low values on the ADC map, suggesting a malignant pathology. Also, borderline pathology is suggested based on conventional MRI, like the presence of vegetation or thick septations and wall.

ADC cut-off of $<1.0\text{x}10^{-3}$ for the solid component of the masses has produced a sensitivity of 90.24%, specificity of 77.78%% with PPV of 94.9%, NPV of 63.6% and accuracy of 88.5% in differentiating malignant from benign masses. (Table: 4)

**Table 4: Comparison of the performance ADC calculation in the current study with literature**

| Author and year of study | ADC cut-off (x10-3 m2/s) | Sensitivity | Specificity |
|---|---|---|---|
| Ahmad et al.15 (2014) | 0.9 | 88.9% | 100% |
| Takeuchi et al.16 (2010) | 1.15 | 74% | 80% |
| Xi et al.2 (2008) | 1.19 | 89.5% | 87.5% |
| Current study | 1.0 | 90.24% | 77.78% |

Semi-quantitative DCE-MRI parameters provide an accurate method for predicting malignancy, particularly in preoperative indeterminate cases. We studied the time/signal intensity curve in addition to semi-quantitative parameters: Tmax, and MRE% to differentiate ovarian masses.

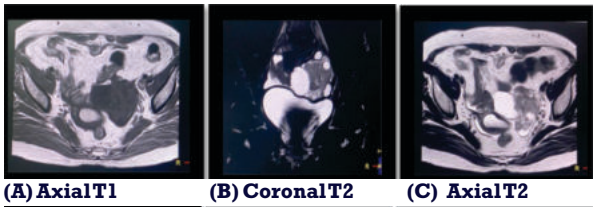

**(A) Axial T1** **(B) Coronal T2** **(C) Axial T2**

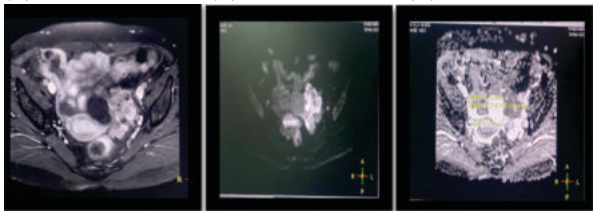

**(D) T1+C** **(E) DWI** **(F) ADC**

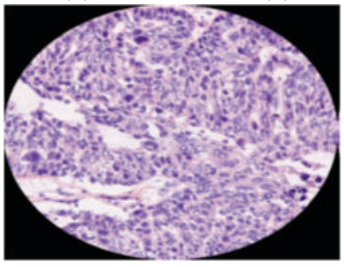

**(H) HPE-High-grade papillary serous cystadenocarcinoma of left ovary**

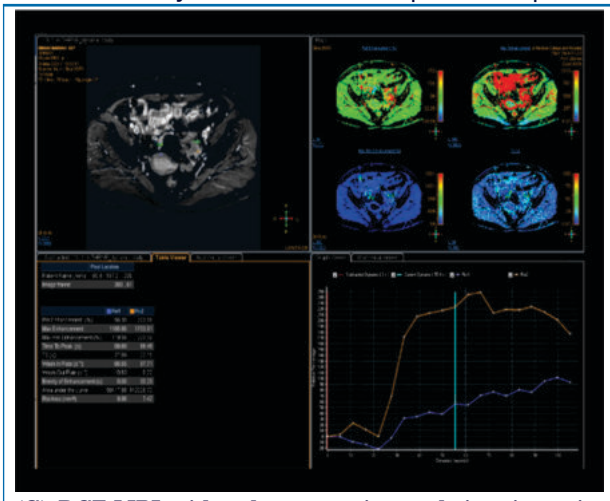

**(G) DCE-MRI with colour mapping and time-intensity curve.**

**Figure 4: Axial and coronal T2WI shows a lobulated left ovarian lesion with irregular solid area, that appear intermediate in signal intensity with peripheral T2 hyperintense cystic components. T1WI shows iso to hypointense signal. T1+C shows heterogenous enhancement. Ascites with peritoneal enhancement seen. DWI shows restriction with a low ADC value. DCE-MR shows a type 3 curve. MRE=223.3%, Tmax=66.4s. T2 hyperintense collection with layering is also seen within the endometrial cavity consistent with hematometra.**

**MRI Diagnosis: Left ovarian O-RADS 5 lesion.**

In our study, 8 (88.9%) out of 9 benign lesions showed a type 1 curve, while one lesion (11.1%) showed type 2 curve. We also had 17 cases of malignant tumors, which demonstrated type 2 curve. 4 (80%) borderline tumors showed type 2 curve. Type 3 curve was only found in malignant lesions (n=18, 50%). (Table: 2)

Our findings are in congruence with a study conducted by Thomassin-Naggara et al. in 2015, where they found that the type 3 curve appeared specific for malignant tumors. Curve type 1 was more frequently found in benign than in malignant tumors. The frequency of curve type 2 was not different amongst the three groups (benign, borderline, and malignant). However, the ability of the curve types to distinguish between benign and borderline tumors was limited since there was an overlap between the curve types of benign and borderline lesions.[17]

Sohaib et al. described that while benign ovarian tumors showed a gradual increase in enhancement without a clearly defined peak, borderline ovarian tumors showed moderate initial enhancement followed by a plateau, and malignant lesions showed greater enhancement than benign lesions during the early phase of enhancement rather than the late phase of enhancement.[18]

As there is an overlap of curve types concerning the histological type, adding semi-quantitative parameters is useful.

In our study, the mean value of time to peak (Tmax) was found to be 154.4±28.3s for benign masses, 121.5±17.1s for borderline and 91.2±28.3s for malignant masses. Malignant masses showed less time to peak (Tmax) than benign and borderline masses.

In this study, optimal Tmax cut-off of ≤145s as a predictor of malignancy has generated a maximum statistical significance (P= 0.001) with a sensitivity of 97.5% and specificity of 70% in comparison to a study conducted by Li et al. in 2017, differentiating malignant and benign ovarian masses on 48 ovarian tumors (13 benign and 35 malignant tumors) investigated the time to peak (Tmax), it yielded a sensitivity of 100% and specificity of 92.31%.[19] (Table: 5)

**Table 5: Diagnostic performance of ORADS-MRI score, Tmax, MRE% and Mean ADC calculation.**

| Parameters | ORADS-MRI score | | Tmax | | MRE% | | Mean ADC of solid components of lesion | |
|---|---|---|---|---|---|---|---|---|
| | Value | 95% CI | Value | 95% CI | Value | 95% CI | Value | 95% CI |
| Sensitivity | 94.74 % | 82.3% to 99.4% | 97.5 % | 86.8% to 99.9% | 80.0 % | 64.4% to 90.9% | 90.24% | 76.9 % to 97.3 % |
| Specificity | 91.67 % | 61.5% to 99.8% | 70.0 % | 34.8% to 93.3% | 80.0 % | 44.4% to 97.5% | 77.78% | 40.0 % to 97.2 % |
| PPV | 97.3 % | 84.6% to 99.6% | 92.9 % | 83.4% to 97.1% | 94.1 % | 82.1% to 98.2% | 94.9 % | 84.4 % to 98.4 % |
| NPV | 84.6 % | 58.5% to 95.5% | 87.5 % | 49.2% to 98.1% | 50.0 % | 33.3% to 66.7% | 63.6 % | 39.3 % to 82.5 % |
| Accuracy | 93.2 % | 82.4% to 98.4% | 87.9 % | 75.4% to 95.4% | 87.6 % | 75.2% to 95.2% | 88.5 % | 76.3 % to 95.8 % |

Another study by Mansour et al. found a sensitivity of 65.7% and specificity of 80.1% taking >200s as the cut-off for the prediction of benignity.[20] In this study, MRE% was higher in malignant (mean value of 148.7 ± 39.6) than in benign lesions (mean value 77.4 ± 46.2) and borderline lesions (mean value 109.6 ± 35.3).

In this study, we found an MRE% cut-off of >118.4 as predictive of borderline/malignancy has yielded a full statistical significance (P=0.001) with a sensitivity of 80 % and specificity of 80%. (Table: 5)

We agree with the study done by Mansour et al. on 150 complex or purely solid ovarian masses evaluating the ability of DCE-MR sequence to diagnose indeterminate ovarian masses, which had shown that MRE% was higher for malignant than for benign and borderline masses (P = 0.001). They obtained a sensitivity of 88% and specificity of 71.4% on taking >122 as the optimal cut-off to predict malignancy.[20] Among the semi-quantitative DCE-MRI parameters in our study, Tmax is more sensitive, and MRE% is more specific, which is consistent with the study done by Kazerooni et al. in 2017.[21] On comparing the with histopathological findings, we found that one ovarian mass was misclassified into O-RADS 3 based on the time/ signal intensity curve. On HPE, it was found to be a malignant adult granulosa cell tumor of the ovary. However, on MRI few intratumoral haemorrhagic foci were seen. (Figure: 5)

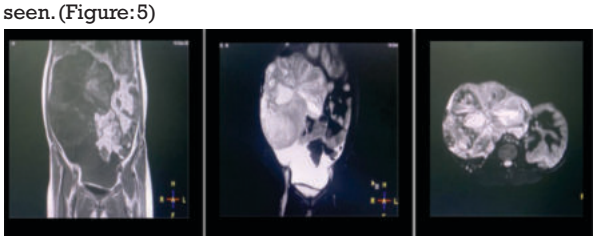

**(A) Coronal T1** **(B) Coronal T2** **(C) DWI**

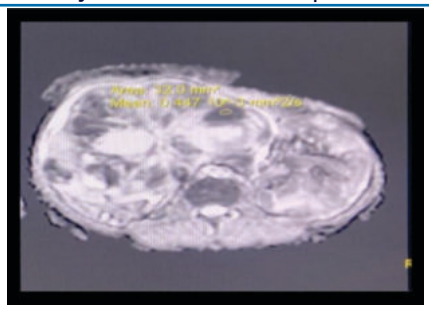

**(D) ADC**

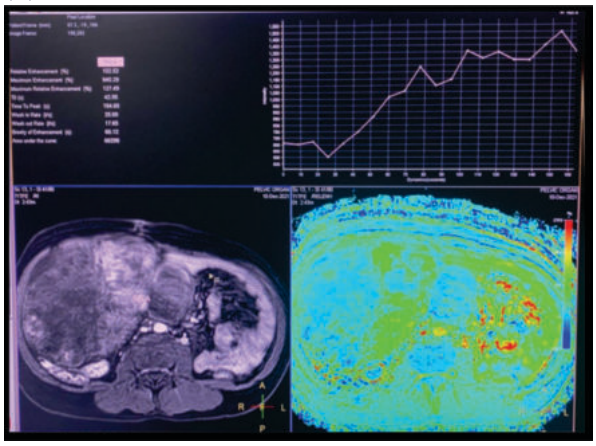

**(G) DCE-MRI with colour mapping and time-intensity curve.**

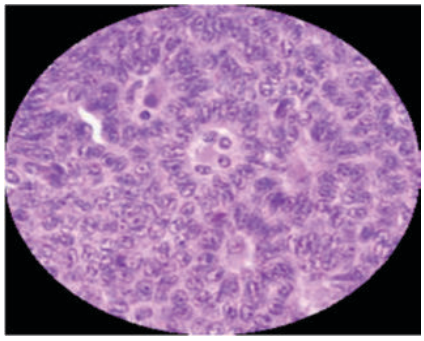

**(H) HPE-Malignant adult granulosa cell tumor of right ovary.**

**Figure 5: Coronal MR images show a large multilocular solid-cystic lesion in the abdomino-pelvic cavity which is heterogenous in signal intensity on T1 and T2WI. Few T1 hyperintense foci are seen, consistent with intratumoral haemorrhage.T1+C shows heterogenous enhancement of the lesion. Ascites seen. DWI shows patchy areas of restricted diffusion with a low ADC value. DCE-MR shows a type 1 curve. MRE=127.4%, Tmax=154.6s,**

**MR Diagnosis: O-RADS 3 lesion.**

Four borderline masses were categorised into O-RADS 4 and one mass into O-RADS 3. The O-RADS 3 lesion was proved borderline serous cystadenoma on HPE.

**Table 6: Distribution of masses according to O-RADS MRI risk score and cross tabulation with HPE findings.**

| O-RADS MRI Score | HPE Category | | | | | | | | p -value |
|---|---|---|---|---|---|---|---|---|---|
| | Benign | | Borderline | | Malignant | | Total | | |
| | No. | % | No. | % | No. | % | No. | % | |
| O-RADS 2 | 1 | 11.10 % | 0 | 0.00 % | 0 | 0.00 % | 1 | 2.00 % | 0.001 |
| O-RADS 3 | 8 | 88.90 % | 1 | 20.0 0% | 1 | 2.80 % | 10 | 20.0 0% | |
| O-RADS 4 | 0 | 0.00% | 4 | 80.00% | 5 | 13.90% | 9 | 18.00% | |
| O-RADS 5 | 0 | 0.00% | 0 | 0.00% | 30 | 83.30% | 30 | 60.00% | |

Our study's ROC curve analysis showed that the accuracy of the O-RADS MRI risk score in detecting malignant masses was 93.2%. The AUC was 0.932. The sensitivity was found to be 94.74%, and the specificity was found to be 93.67%. The PPV and NPV are 97.3% and 84.6%, respectively. (Table: 7)

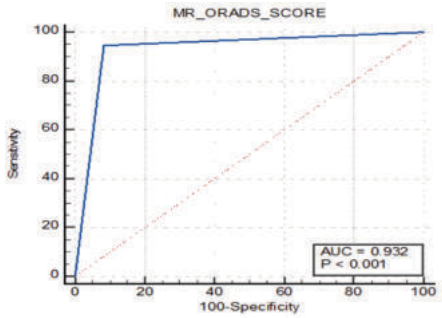


**Figure 6: ROC curve analysis for "O-RADS MRI risk score" with HPE as the gold standard.**

**Table 7: Comparison of the performance O-RADS MRI risk score in the current study with literature.**

| Author and year of study | O-RADS MRI/ ADNEX MR | Sensitivity | Specificity |
|---|---|---|---|
| Thomassin-Naggara et al.[9] (2020) | O-RADS MRI | 93% | 91% |
| Pereira et. al.[22] (2022) | O-RADS MRI | 91.11% | 94.92% |
| Sasaguri et. al.[23] (2018) | ADNEX MR | 85.6% | 90.1% |
| Basha et. al[24] (2020) | ADNEX MR | 94.9% | 92.9% |
| Our study | O-RADS MRI | 94.74% | 93.67% |

In our study, surface epithelial tumors were the most common. They constituted 80% of the masses, comparable with the findings of Gupta et al.[25] and Pilli et al.[26] Serous cystadenocarcinoma (Figure: 4) was the most common malignant ovarian mass (n=18, 36%) followed by mucinous cystadenocarcinoma. 36 out of 50 lesions were proved malignant on HPE. This is largely because we included only indeterminate and suspicious ovarian masses in our study. Germ cell tumors constituted 2%, sex cord-stromal tumors 6% and krukenberg (Figure: 7) constituted 4% of the masses.

**Table 8: Distribution based on different histopathological diagnoses of the masses.**

| | Benign | Borderline | Malignant |
|---|---|---|---|
| Surface Epithelial tumors | Serous cysta-denoma (n=2) | Borderline Serous cysta-denoma (n=2) | High-grade serous cystadeno-carcinoma (n=18) |
| | Mucinous cystadenofib roma (n=1) | | Mucinous cystadenocarcino ma (n=10) |
| | Benign Brenner tumor (n=1) | Borderline Mucinous cystadenoma (n=3) | Clear cell carcinoma (n=1) |
| | | | Endometrioid carcinoma (n=2) |
| Germ cell tumors | | | Ovarian dysgerminoma (n=1) |
| Sex cord-stromal tumors | Fibroma (n=1) | | Adult granulosa cell tumor of ovary (n-2) |
| Metastas es | | | Krukenberg tumor (n=2) |

| | | | |
|---|---|---|---|
| Inflammatory | Haemorrhagic cyst (n=1) | | |
| | Tubo-ovarian abscess (n=2) | | |
| | Broad ligament fibroid (n=1) | | |

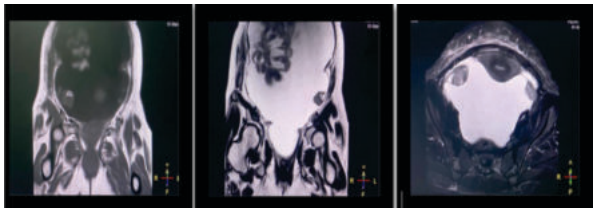

**(A) Axial T1** **(B) Coronal T2** **(C) Axial T2**

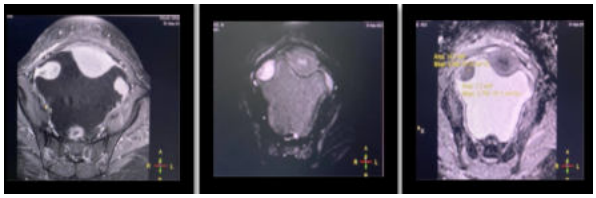

**(D) T1+C** **(E) DWI** **(F) ADC**

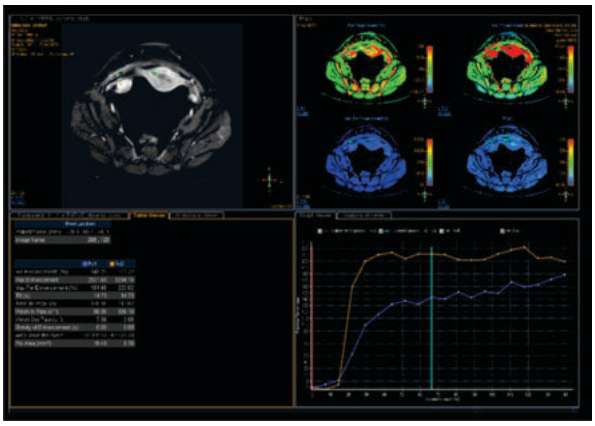

**(G) DCE-MRI with colour mapping and time-intensity curve.**

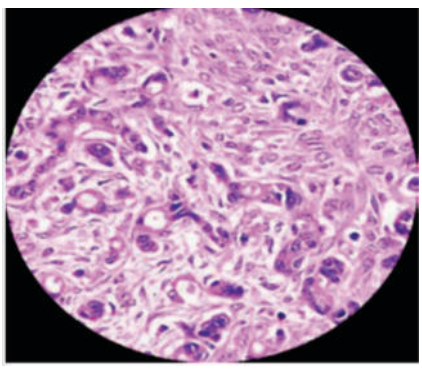

**(H) HPE-Krukenberg tumor of bilateral ovaries.**

**Figure 7: Axial and coronal and T2WI images show bilateral solid ovarian masses showing intermediate signal intensity. T1+C shows vivid enhancement of the lesions along with enhancing peritoneal thickening. Moderate ascites seen. DWI shows restriction with a low ADC value. DCE-MR shows a type 3 curve. MRE=220.8%, Tmax=117.8s. MRI Diagnosis: Bilateral O-RADS 5 lesions.**

## CONCLUSION:

Due to the wide range of differential diagnoses and complex appearance, there is a delay in diagnosing ovarian and adnexal masses, which increases mortality. Treatment of patients with ovarian masses necessitates initial risk categorization based on the radiological and imaging appearance of the mass, clinical presentation, and serum CA-125 level. Identifying the imaging characteristics of benign and malignant ovarian masses can alter therapeutic options available to the patient depending on the age group. Ultrasound is the primary modality in evaluating adnexal and ovarian lesions, while MRI is reserved for sonographically indeterminate cases. DWI and DCE-MRI, in conjunction with conventional MRI plays a vital role in the characterization of indeterminate and suspicious ovarian lesions. Functional MRI is currently a possible predictive and prognostic biomarker in ovarian lesions. Functional MRI helps to discriminate benign ovarian lesions from borderline and malignant lesions based on DCE-MRI parameters. DWI can confirm or exclude potential malignancy in complex ovarian masses, provided inclusion of the conventional MRI data, combined analysis of DWI quantitative and qualitative criteria, and awareness of the possible sequence pitfalls.

In our study, the mean ADC value of solid components of the masses and semi-quantitative DCE parameters: Tmax and MRE%, were proved to have good diagnostic performance. However, the best agreement was noted between the O-RADS MRI risk score and the final HPE diagnosis. We conclude that in cases of indeterminate ovarian masses in sonography, MRI should be the investigation of choice with the addition of functional MR sequences, like DWI and DCE-MRI. Further, applying the O-RADS MRI risk score in clinical practice may allow for a customized patient-centred strategy for sonographically indeterminate masses.

## REFERENCES


1. https://gco.iarc.fr/today/data/factsheets/populations/356-india fact sheets.pdf.
2. Pi S, Cao R, Qiang JW, Guo YH. Utility of DWI with quantitative ADC values in ovarian tumors: a meta-analysis of diagnostic test performance. Vol. 59, Acta Radiologica. SAGE Publications Inc.; 2018. p. 1386–94.
3. Van Calster B, Timmerman D, Valentin L, McIndoe A, Ghaem-Maghami S, Testa AC, et al. Triaging women with ovarian masses for surgery: Observational diagnostic study to compare RCOG guidelines with an international ovarian tumor Analysis (IOTA) group protocol. BJOG. 2012;119(6).
4. Timmerman D, Ameye L, Fischerova D, Epstein E, Melis GB, Guerriero S, et al. Simple ultrasound rules to distinguish between benign and malignant adnexal masses before surgery: Prospective validation by IOTA group. BMJ. 2011;342(7788).
5. Kim S, Loevner L, Quon H, Sherman E, Weinstein G, Kilger A, et al. Diffusion-Weighted Magnetic Resonance Imaging for Predicting and Detecting Early Response to Chemoradiation Therapy of Squamous Cell Carcinomas of the Head and Neck. Available from: http://clincancerres.aacrjournals.org/
6. McVeigh PZ, Syed AM, Milosevic M, Fyles A, Haider MA. Diffusion weighted MRI in cervical cancer. Eur Radiol. 2008;18(5).
7. Staats PN, Young RH. Sex Cord-Stromal, Steroid Cell, and Other Ovarian Tumors with Endocrine, Paraendocrine, and Paraneoplastic Manifestations. In: Blaustein's Pathology of the Female Genital Tract. 2019.
8. O-RADSTM MRI Risk Stratification System O-RADS MRI Risk Score Governing Concepts. 2020. (https://www.acr.org/-/media/ACR/Files/RADS/O-RADS/O-RADS-MR-Risk-Stratification-System-Table-September-2020.pdf)
9. Thomassin-Naggara I, Poncelet E, Jalaguier-Coudray A, Guerra A, Fournier LS, Stojanovic S, et al. Ovarian-Adnexal Reporting Data System Magnetic Resonance Imaging (O-RADS MRI) Score for Risk Stratification of Sonographically Indeterminate Adnexal Masses. JAMA Netw Open. 2020 Jan 24;3(1).
10. Sohaib SAA. MR imaging in ovarian cancer. Cancer Imaging. 2007;7(Special Issue A):S119–29.
11. Brown DL, Zou KH, Tempany CM, Frates MC, Silverman SG, McNeil BJ, et al. Primary versus secondary ovarian malignancy: imaging findings of adnexal masses in the Radiology Diagnostic Oncology Group Study. Radiology. 2001 Apr;219(1):213–8.
12. Elzayat WA, El-Kalioubie M, Abdel-Naby MM, Abdel-Malek RR. The role of dynamic contrast enhanced MR imaging in the assessment of inconclusive ovarian masses. The Egyptian Journal of Radiology and Nuclear Medicine. 2017 Dec;48(4):1159–69.
13. Li W, Chu C, Cui Y, Zhang P, Zhu M. Diffusion weighted MRI: a useful technique to differentiate benign versus malignant ovarian surface epithelial tumors with solid and cystic components. Abdom Imaging. 2012 Oct;37(5):897-903
14. Thomassin-Naggara I, Daraï E, Cuenod CA, Fournier L, Toussaint I, Marsault C, et al. Contribution of diffusion-weighted MR imaging for predicting benignity of complex adnexal masses. Eur Radiol. 2009 Jun;19(6):1544–52
15. Ahmad KA, Abdrabou A. The significance of added ADC value to conventional MR imaging in differentiation between benign and malignant ovarian neoplasms. The Egyptian Journal of Radiology and Nuclear Medicine. 2014 Sep;45(3):997–1002
16. Takeuchi M, Matsuzaki K, Nishitani H. Diffusion-weighted magnetic resonance imaging of ovarian tumors: differentiation of benign andmalignant solid components of ovarian masses. J Comput Assist Tomogr. 34(2):173–6
17. Thomassin-Naggara I, Balvay D, Rockall A, Carette MF, Ballester M, Darai E, et al. Added Value of Assessing Adnexal Masses with Advanced MRI Techniques. Biomed Res Int. 2015;2015:1–10
18. Sohaib SAA, Sahdev A, van Trappen P, Jacobs IJ, Reznek RH. Characterization of adnexal mass lesions on MR imaging. AJR Am J Roentgenol. 2003 May;180(5):1297–304

19. Li HM, Qiang JW, Ma FH, Zhao SH. The value of dynamic contrast–enhanced MRI in characterizing complex ovarian tumors. J Ovarian Res. 2017 Dec 14;10(1):4.
20. Mansour SM, Saraya S, El-faissal Y. Semi-quantitative contrast enhanced MR analysis of indeterminate ovarian tumors: when to say malignancy? Br J Radiol. 2015 Sep;88(1053):20150099
21. Kazerooni AF, Malek M, Haghighatkhah H, Parviz S, Nabil M, Torbati L, et al. Semiquantitative dynamic contrast-enhanced MRI for accurate classification of complex adnexal masses. J Magn Reson Imaging. 2017;45(2):418–27
22. Pereira PN, Yoshida A, Sarian LO, Barros RH de O, Jales RM, Derchain S. Assessment of the performance of the O-RADS MRI score for the evaluation of adnexal masses, with technical notes. Radiol Bras. 2022 May;55(3):137–44.
23. Sasaguri K, Yamaguchi K, Nakazono T, Mizuguchi M, Aishima S, Yokoyama M, et al. External validation of ADNEX MR SCORING system: a single-centre retrospective study. Clin Radiol. 2019;74(2):131–9
24. Basha MAA, Abdelrahman HM, Metwally MI, Alayouty NA, Mohey N, Zaitoun MMA, et al. Validity and Reproducibility of the ADNEX MR Scoring System in the Diagnosis of Sonographically Indeterminate Adnexal Masses. J Magn Reson Imaging. 2021;53(1):292–304
25. Gupta N, Bisht D, Agarwal AK, Sharma VK. Retrospective and prospective study of ovarian tumors and tumor-like lesions. Indian J Pathol Microbiol. 2007 Jul;50(3):525–7
26. Pilli GS, Suneeta KP, Dhaded A v, Yenni V v. Ovarian tumors: a study of 282 cases. J Indian Med Assoc. 2002 Jul;100(7):420, 423–4, 447